

# Pressure Sensitive Adhesives Based on Epoxidized Soybean Oil: Correlation Between Curing Conditions and Rheological Properties

Emiliano M. Ciannamea<sup>1</sup> · Roxana A. Ruseckaite<sup>1</sup>

Received: 29 November 2017 / Revised: 17 January 2018 / Accepted: 23 January 2018  
© 2018 AOCS

**Abstract** Renewable resources, including vegetable oils, can be used as feedstock for the manufacture of *pressure sensitive adhesives (PSA)* that can compete with those derived from petrochemical sources, but with the environmental benefit of being sustainable. Completely bio-based PSA with tunable viscoelastic properties were synthesized from mixtures of epoxidized soybean oil and sebacic acid by a solvent-free one-step reaction, in the absence of catalyst. Curing conditions and pot-life were determined for formulations with stoichiometric acid/epoxy ratio. Curing time ranged from the gel point ( $t_{gel}$ ) to  $t_{gel} + 30$  min at the selected temperature (170 °C) to study the correlation between the reaction, rheological behavior, and potential adhesive performance. These renewable PSA can be tailored by controlling the curing parameters according to the desired application, since the rheological profile and gel content were greatly dependent on the curing conditions. In particular, the obtained adhesives cured at 170 °C between 65 and 75 min showed the best balance between tack and cohesion.

**Keywords** Sebacic acid · Renewable · Bio-based · Dicarboxylic acids · Viscoelastic properties

*J Am Oil Chem Soc* (2018) 95: 525–532.

✉ Emiliano M. Ciannamea  
emiliano@fi.mdp.edu.ar

<sup>1</sup> Instituto de Investigaciones en Ciencia y Tecnología de Materiales (INTEMA), Universidad Nacional de Mar del Plata—CONICET, Avenida Juan B. Justo 4302, B7608FDQ, Mar del Plata, Argentina

## Introduction

Pressure-sensitive adhesives (PSA) are a special category of polymeric materials that are permanently tacky at the operating temperature and can adhere to any given substrate under slight pressure in a very short time (Maaßen et al., 2015; Wool, 2013; Wu, Li, & Li, 2015). PSA differ from other adhesives since they can act at room temperature via noncovalent forces without any chemical reaction, phase change (liquid to solid), or solvent evaporation (Cohen, Binshatok, Dotan, & Dodiuk, 2013; Creton, 2003; Vendamme et al., 2012; Wu, Li, & Li, 2014). These kinds of adhesives have applications in many fields, such as tapes, labels, protection films, and so on, especially in the electric, automotive, packing, and medical industries (Li & Sun, 2014).

The behavior of PSA depends on a perfect balance between viscous and elastic properties (Torron, Hult, Pettersson, & Johansson, 2017). Liquid-like dissipative character is necessary to deform (or flow) and quickly wet the substrate surface under light pressure to establish molecular contact and generate tack (adhesion). Solid-like behavior is required to resist flow during a separation or debonding process and to sustain loads (cohesion) (Cohen et al., 2013; Li & Li, 2014a, 2014b). The viscoelasticity of PSA is also responsible for the phenomena of cavitation and fibril formation that are fundamental for the dissipation of mechanical stresses during the debonding step and the modulation of the adhesive force (Vendamme et al., 2012). Polymers used in PSA formulations are typically linear with a slight degree of cross-linking and low glass transition temperature ( $T_g$ ). PSA properties can be tailored by controlling the balance between the cohesive and adhesive strengths of the polymer, in order to achieve the desired

and optimum proportion of tack, peel, and shear strength according to the intended application (i.e., permanent or completely removable). The degree of cross-linking, sol/gel fraction,  $T_g$ , and molecular weight distribution are the key features in the control of PSA performance (Maaßen et al., 2015; Maassen, Meier, & Willenbacher, 2016; Vendamme et al., 2012; Wool, 2013).

Except for natural rubbers, current PSA are predominantly made from petroleum-based polymers (acrylics, silicones, copolymers, and so on). Renewable resources, including vegetable oils, can also be used as feedstocks for the manufacture of PSA that can compete with those derived from petrochemical sources, but with the environmental benefit of being sustainable (Ding & Matharu, 2014; Li & Li, 2014a; Li & Sun, 2014; Vendamme et al., 2012; Wang, Chen, Wu, Fu, & Wang, 2017; Wu et al., 2015; Wu & Li, 2017). Plant oils and fatty acids offer many attractive advantages apart from their renewability, including their worldwide availability and relatively low prices. Most importantly, only minor modification reactions have to be performed to obtain a variety of polymer precursors for many different applications (de Espinosa & Meier, 2011).

The recent advances on sustainable PSA from vegetable oils, fatty acids, and polyols (derived from vegetable and/or animal fats and oils) (Li & Li, 2014a, 2014b, 2015; Li et al., 2017; Li & Sun, 2014; Li, Wang, & Sun, 2015; Maassen et al., 2016; Wu et al., 2015) evidence the potential of these renewable feedstocks as PSA precursors. Epoxidized soybean oil (ESO) and epoxidized fatty acids were cured with natural dicarboxylic acids (Li & Li, 2014a, 2014b; Li et al., 2015) and phosphoric acid (Ahn, Sung, Kim, Kraft, & Sun, 2013) or phosphorous-containing dicarboxylic acids (Wang et al., 2017) to afford hydroxyl-functionalized polymers with suitable adhesion properties. Hydroxyl-functionalized polyesters obtained from the step-growth polymerization of bifunctional monomers derived from methyl oleate were cured with ESO or trimethylolpropane triglycidyl ether (Wu et al., 2014) or polymeric methylene diphenyl diisocyanate (Wu et al., 2015) to give PSA with high peel strength, tack force, aging resistance, and thermal stability. Maleinized tung oil polymerized with a variety of diols produced cross-linked acid-functionalized polyesters with good peel strength and aging resistance (Li & Li, 2015; Wu et al., 2014, 2015). Acrylic polyols synthesized from ESO with controlled degree of acrylation and hydroxyl functionality were radically cured to obtain polymers with a good balance of flexibility and cross-linking, suitable for PSA applications (Li & Sun, 2015).

The motivation of this study was the design and characterization of completely renewable PSA with tunable properties through environmentally sustainable processes. ESO–sebacic acid (SA)-based PSA were produced in the absence of catalyst or solvents and characterized.

Viscoelastic and adhesive properties of the materials were studied and tailored by controlling the reaction conditions.

## Experimental Section

### Materials

ESO with an epoxy equivalent weight = 241.2 g eq<sup>-1</sup> and iodine value = 2.4 was kindly supplied by Unipox (Buenos Aires, Argentina). SA, with a melting point  $T_m = 134.9$  °C, was obtained from Castor Oil (Buenos Aires, Argentina). Dry toluene was purchased from Sigma–Aldrich (St Louis, MO, USA).

### ESO–SA Mixture Preparation

Mixtures of ESO and SA at stoichiometric –COOH/epoxy ratios ( $R = 1$ ) were prepared in a 25 mL glass vial equipped with a magnetic stirrer. The reactor was placed in a thermostat at 140 °C for 15 min. Mixtures were kept in refrigerator at 4 °C before use.

### ESO–SA Adhesives Preparation

Curing was performed by pouring about 2 g of freshly prepared ESO–SA reactive mixtures in silicone molds (diameter 7 cm) and then stabilized at 50 °C for 15 min in a convection oven (Yamato DKN400; Santa Clara, CA, USA). Subsequently, specimens were subjected to a two-step curing process selected from preliminary differential scanning calorimeter (DSC) and pot-life studies: heating from 50 °C to the desired curing temperature (i.e., 170 °C) at 5 °C min<sup>-1</sup>, followed by an isothermal step for a specific lapse of time (45–85 min). Different curing times were evaluated considering the gel time ( $t_{gel}$ ), previously determined by rheological studies.

### Characterization

DSC experiments were carried out in a DSC Shimadzu DSC50 (Kyoto, Japan) under nitrogen atmosphere (20 cm<sup>3</sup> min<sup>-1</sup>). Reactive ESO–SA mixtures (7–10 mg) were poured into aluminum pans and subjected to a programmed cycle: heating from room temperature up to 250 °C at a heating rate of 10 °C min<sup>-1</sup>, rapid cooling to room temperature, and reheating up to 250 °C at 10 °C min<sup>-1</sup>. Curing reaction parameters, such as enthalpy of reaction ( $\Delta H_r$ ) and temperature peak ( $T_p$ , defined as the maximum of the reaction peak), were taken from the first run. ESO–SA adhesives (cured samples) were analyzed by dynamic DSC tests from –60 to 250 °C at a heating rate of 10 °C

$\text{min}^{-1}$  under nitrogen atmosphere by using the same calorimeter and glass transition temperature ( $T_g$ ) was taken as the midpoint of the transition. Isothermal DSC experiments were carried out on ESO–SA mixtures at 160, 170, and 180 °C, until the heat signal was invariant. Samples were cooled to room temperature and, to ensure that the maximum conversion was reached, specimens were submitted to a reheating step up to 250 °C at 10 °C  $\text{min}^{-1}$ . The obtained isothermal curves were integrated and the reaction conversion as a function of time was calculated as

$$\alpha(t) = \frac{A(t)}{A_\infty} \times 100 \quad (1)$$

where  $\alpha(t)$  is the extent of the reaction at time  $t$ ,  $A(t)$  is the area under the curve at time  $t$ , and  $A_\infty$  is the area under the curve at infinite time. The instrument was calibrated with high-purity indium at 10 °C  $\text{min}^{-1}$ , following the standard procedure.

Fourier-transform infrared spectroscopy (FTIR) spectra of ESO–SA mixtures and ESO–SA-based PSA were recorded on a Thermo Scientific Nicolet 6700 spectrometer (Waltham, USA) equipped with an attenuated total reflectance (ATR) module with a diamond crystal, performing 64 scans at room temperature, using a resolution of 2  $\text{cm}^{-1}$ , between 4000 and 650  $\text{cm}^{-1}$ .

Pot-life of ESO–SA mixtures was determined following the procedure reported elsewhere (Wu & Li, 2016), with some modifications. Oscillatory test was performed with an Anton Paar MCR 301 rheometer (Graz, Austria) with parallel plate geometry with a diameter of 25 mm and a gap of 0.4 mm. First, samples were equilibrated at 50 °C for 15 min. At time zero, temperature was raised up to the desired value (160–180 °C) at a heating rate of 5 °C  $\text{min}^{-1}$ . Frequency was set at 0.5 Hz, and strain amplitude of 50% and a sampling time of 1 s were used. Similar geometry was used to characterize ESO–SA cured samples. Frequency sweep measurements were performed for cured samples at 25 °C from 0.01 to 100 Hz, using a 0.1% of strain.

Gel content was determined by immersing an accurately weighted (0.5 g,  $\pm 0.0001$ ,  $m_i$ ) amount of cured ESO–SA sample in 15 mL of dry toluene in preweighted glass vials and let stand in the dark at room temperature for 10 days. Solvent was removed by rotator evaporation and the remaining solid (gel) was dried in air-convection oven at 105 °C until constant weight ( $\pm 0.0001$ ,  $m_d$ ). The gel content was calculated as  $m_d/m_i \times 100$ . All measurements were performed in triplicate.

## Results and Discussion

### Study of ESO–SA Mixtures: Selection of Curing Conditions

Dicarboxylic acids have been demonstrated to efficiently cross-link epoxidized oils and epoxidized fatty acids (Ding,

Shuttleworth, Makin, Clark, & Matharu, 2015; Li & Li, 2014b, 2015; Wu et al., 2015), particularly in the presence of catalysts. However, their use as curing agents is poorly explored, possibly because epoxy-carboxylic acid reactions are quite complex, since esterification, condensation, transesterification, and hydrolysis are all possible (Auvergne Rm, David, Boutevin, & Pascault, 2013; Ding et al., 2015).

The ESO–SA curing process in the absence of catalyst was analyzed by nonisothermal DSC. The thermogram revealed a first broad endothermic peak (80–135 °C), with a minimum at around 120 °C, assigned to the melting of SA ( $T_m = 134.9$  °C, measured in pure SA) followed by a single exothermic event peaking at 203.3 °C, associated with the ESO–SA curing reaction (Ding et al., 2015). The total enthalpy released during curing reaction ( $\Delta H_c$ ) was close to 21.2 J  $\text{g}^{-1}$ , which was in the same range as values previously reported for ESO–SA in the presence of 1-methyl imidazole (catalyst) (Mashouf Roudsari, Mohanty, & Misra, 2014) and epoxidized linseed oil cured with dicarboxylic acid in the presence of 4,4'-dimethylaminopyridine (Ding et al., 2015), but significantly lower when compared with the enthalpy currently encountered for Bisphenol A diglycidyl ether (DGEBA)-carboxylic acids (Mashouf Roudsari et al., 2014). This was ascribed to the hindered oxirane functionalities, which were in the middle of the fatty acids in the ESO molecule and reacted sluggishly with nucleophilic curing agents in the stoichiometrically balanced polymerizations (Altuna, Espósito, Ruseckaite, & Stefani, 2011; Mashouf Roudsari et al., 2014). No additional transitions were observed during a second scan, verifying the completeness of the curing reaction during the first scan up to 250 °C.

Conversion vs. time curves are very helpful in determining the minimum time to complete the curing reaction for a given temperature. As shown in Fig. 1, higher curing

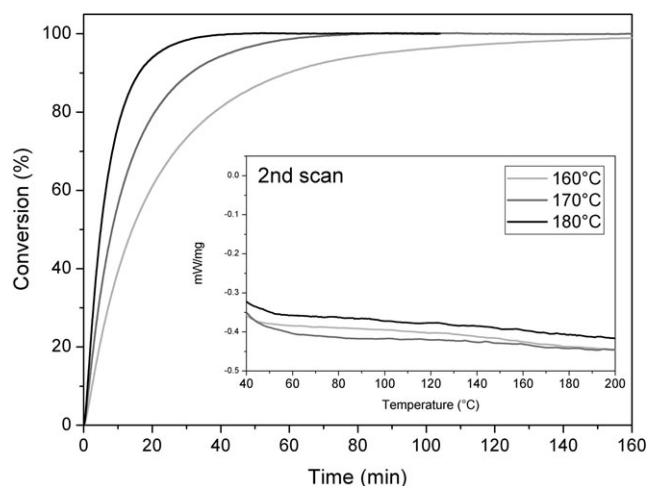
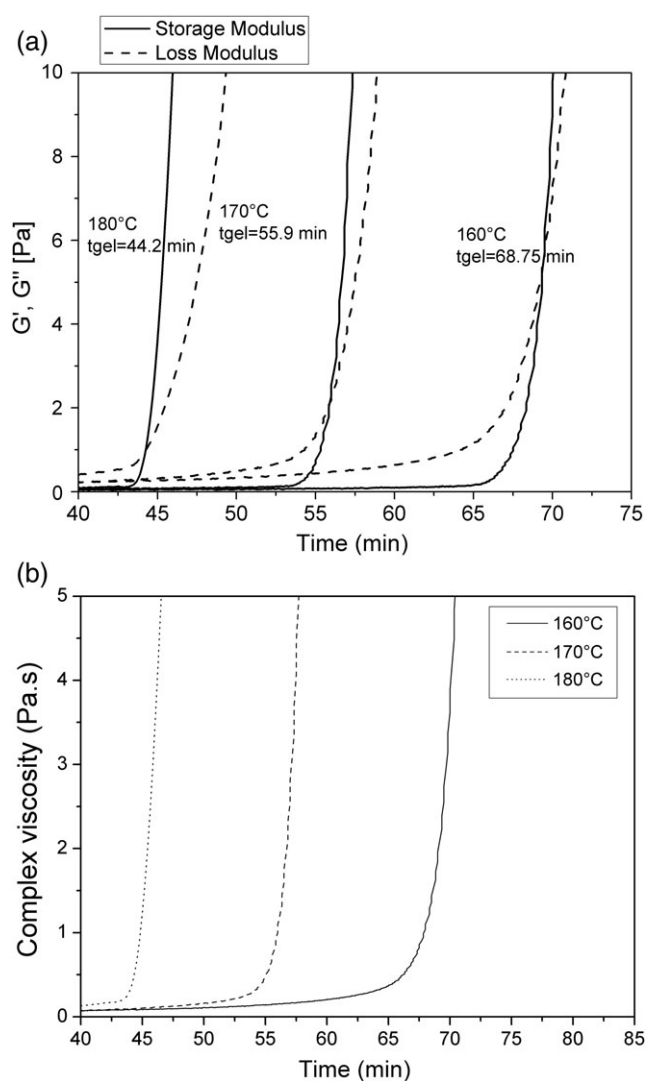


Fig. 1 Conversion of ESO–SA at different curing temperatures

temperatures resulted in greater reaction rates (see the slope of curves); i.e., at 180 °C sample attained 98% of conversion in approximately 28 min, while curing at 160 °C enlarged the time up to 131 min. Lower curing temperatures (i.e., 140, 150 °C, data not shown) resulted in longer reaction times, limiting the application of the PSA under actual conditions. No residual exothermal peaks were detected in a second dynamic scan in any of the studied cases (no residual curing heat), so it can be assumed that the maximum conversion was reached.

Oscillatory tests were performed at 160, 170, and 180 °C (Fig. 2) to determine the time necessary for ESO–SA reactive mixtures to gel. Initially, the sample was in liquid state with a loss modulus ( $G''$ ) higher than the storage modulus ( $G'$ ) (Fig. 2a). By increasing the curing extent, the complex viscosity and  $G'$  suddenly increased and  $G'$  prevailed over



**Fig. 2** (a) Pot life curves of ESO-SA samples at different curing temperatures. *Solid lines: Storage modulus; Dash lines: Loss Modulus* and (b) viscosity of ESO-SA samples at different curing temperatures

$G''$  at gelation ( $\tan \delta = 1$ ), the so-called sol–gel transition (Maassen et al., 2016; Vendamme & Eevers, 2013). The time when both modulus crossover,  $G' = G''$ , was considered as the gel point ( $t_{gel}$ ; Fig. 2a) (Creton, 2003; Maassen et al., 2016). As expected, gelation took place earlier with increasing the curing temperature. Viscosity values of liquid mixtures (initial viscosity) were between 0.08 and 0.13 Pa s, being in the same range of commercial styrenated liquid resins (viscosity 0.05–6 Pa s) (Wu & Li, 2017). From calorimetric and rheological experiments, 170 °C was targeted as the curing temperature ( $t_{gel} = 55.9$  min).

### Characterization of ESO–SA-Based Adhesives: Effect of the Reaction Time Vs. Rheological Behavior and Potential Adhesive Performance

It has been reported that the optimum degree of cross-linking for PSA applications is found slightly above the gel point (Creton, 2003). Accordingly, curing time ranged from  $t_{gel}$  to  $t_{gel} + 30$  min at the selected temperature (170 °C) to study the correlation between the reaction, final rheological, and potential adhesive performance.

ATR-FTIR was used to get a better understanding of the reaction between ESO and SA (Fig. 3) at the selected curing temperature. The most significant bands in the initial ESO–SA reactive mixture were detected at 3500  $\text{cm}^{-1}$  (OH stretching), 2920 and 2852  $\text{cm}^{-1}$  ( $\text{CH}_2$  stretching), 1739  $\text{cm}^{-1}$  (stretching  $\text{C}=\text{O}$  ester moiety), 1690  $\text{cm}^{-1}$  (stretching  $\text{C}=\text{O}$  of  $-\text{COOH}$  groups) (Ding et al., 2015; Li & Li, 2014b) and the absorption peaks associated with C–O stretching vibrations of the internal oxirane rings in ESO at 820–840  $\text{cm}^{-1}$  (Altuna et al., 2011). The progress of the curing reaction was characterized by the reduction of the oxirane and carboxylic acid absorption peaks (inset of

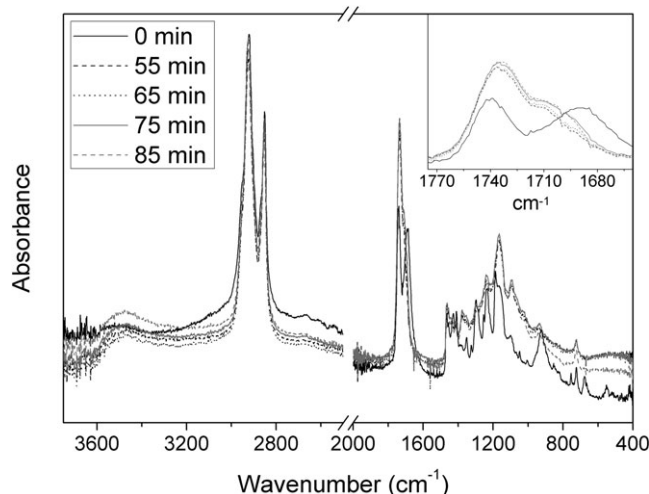


**Fig. 3** ATR-FTIR spectra of unreacted and cured ESO-SA samples

Fig. 3) (Torrón et al., 2017; Zeng, Wu, Li, Wang, & Zeng, 2017), with the concomitant relative increment in the intensity of the bands at 1735 and 3500  $\text{cm}^{-1}$ , evidencing the formation of new ester linkages and secondary (beta) OH groups, leading to the formation of hydroxyl-functionalized branched oligomeric chains (Ahn, Kraft, Wang, & Sun, 2011; Li & Li, 2014a, 2014b; Wu et al., 2015; Zeng et al., 2017). Higher reaction times (i.e., 75–85 min) led to the complete disappearance of the epoxy bands and slight increase of the ester peak, suggesting the complete curing reaction (Zeng et al., 2017), at least within the detection limit of this method. After curing, a shoulder at the right of ester band related with  $-\text{COOH}$  groups was still present. Li and Li (2014a) suggested that epoxy groups were consumed faster than the  $-\text{COOH}$  groups throughout the polymerization since epoxy groups are probably involved in side reactions with secondary  $-\text{OH}$  and water (Li & Li, 2014b). It has been reported that the presence of  $-\text{OH}$  and  $-\text{COOH}$  groups in the polymerized product could both improve the adhesion strength of the PSA by developing hydrogen bonds and other noncovalent interactions with the substrate, and also contribute to the cohesion of the adhesive by enhancing interchain cohesion between the networks and/or sol fractions via intermolecular hydrogen bonding interactions (Li & Li, 2014a).

Glass transition temperature values of ESO–SA at 170 °C for different periods of time ranged between  $-10.2$  and  $-19.0$  °C (Table 1), in the same trend with data reported recently for ESO–dicarboxylic acid systems (Li et al., 2017; Mashouf Roudsari et al., 2014; Zeng et al., 2017). The  $T_g$  of the PSA needs to be lower than the temperature intended to be used at, so the polymer segment can move and the material has its greatest ability to lose energy through deformation and possess enough tackiness (Li & Li, 2014a; Li et al., 2017). However, if the  $T_g$  is too low, the PSA will probably have poor cohesion (Li et al., 2017). Since in practice the PSA is intended to be used at room temperature, the  $T_g$  of the adhesive must be 25–45 °C below that temperature, in accordance with obtained results (Creton, 2003; Li & Li, 2014a).

Control over the sol/gel content is a key parameter for the design of functional PSA and is related to the ability of the material to dissipate energy through deformation (Ahn et al., 2011; Vendamme & Eevers, 2013; Wang et al.,

2017). Gel content of ESO–SA samples cured at 170 °C for different periods of time was measured to confirm the cross-linking nature of the obtained products. Short-time cured samples (45 and 55 min) were totally and 90% soluble, respectively, after 10 days of immersion in dry toluene, probably due to the formation of soluble branched products, as reported in early studies (Zeng et al., 2017). Conversely, samples cured for 65–85 min (above gel point,  $t_{\text{gel}} = 55.9$  min) exhibited significant higher gel fraction varying from  $63.3 \pm 3.0$  to  $70.5 \pm 0.2\%$ , confirming the formation of a cross-linked polymer network in agreement with rheological studies (Li & Li, 2014a).

The correlation between the bulk viscoelastic properties of PSA and their adhesion performance has been well established (Chang, 1991; Li & Sun, 2015; Wang et al., 2017). Characterization of linear viscoelastic properties of cured ESO–SA ( $R = 1$ ) samples (Fig. 4) was conducted by using frequency sweep measurements at fixed room temperature (25 °C, from 0.01 to 100 Hz, using a 0.1% of strain). In an oscillatory frequency sweep, the lower frequencies (i.e., 0.01 Hz) characterize the bond formation and shear behavior since the adhesive can flow and wet the substrate under gentle pressure, whereas higher frequencies (100 Hz) refer to peel or quick-stick properties (debonding) (Vendamme & Eevers, 2013; Wang et al., 2017). In general, a good performance PSA should have a low bonding plateau modulus at the bonding frequency and high energy dissipation at the debonding frequency. As shown in Fig. 4, both moduli increased with frequency, reaching a maximum storage modulus meeting the Dahlquist's criterion, which states that a PSA needs to have a plateau modulus lower than  $10^5$  Pa, so it can wet a rough substrate surface to form a good bond under a light pressure (Gay & Leibler, 1999; Li & Sun, 2015; Wu et al., 2015). The transition from lower to higher modulus ensures good wettability during the bonding process and good cohesive strength during debonding (Torrón et al., 2017). Specimens cured at shorter times, such as 45 and 55 min, performed as viscous liquids ( $G'' > G'$ ) in the entire frequency range (45 min, data not shown), being very tacky at touching with the formation of numerous fibrils when debonding. This observation was in line with the low degree of cross-linking attained by these samples (gel content = 0–10%), and confirmed by seeing the Cole–Cole plot (Fig. 5), where the curve is located in the left side of the equimoduli limit in the complete range, denoting their viscous character (Vendamme et al., 2012).

Increasing curing time, i.e., 65 min ( $t_{\text{gel}} + 10$  min), gave rise to sticky and cohesive gels. This formulation was aggressively tacky at touching and fibrils were formed when debonding, but to a significantly lesser extent than for 55 min cured samples. Samples cured for 65 min exhibited a frequency-dependent behavior: elastic behavior ( $G' > G''$ ) at low frequencies, a crossover ( $G' = G''$ ) at approximately 1 Hz, and viscous behavior at high

**Table 1** Gel content of cured ESO–SA samples

Time (min)	$T_g$ (°C)	Gel content (%)
45	$-19.0$	$1.0 \pm 0.2$
55	$-15.9$	$9.4 \pm 3.5$
65	$-14.3$	$63.3 \pm 3.0$
75	$-11.7$	$66.2 \pm 0.7$
85	$-10.2$	$70.5 \pm 0.2$

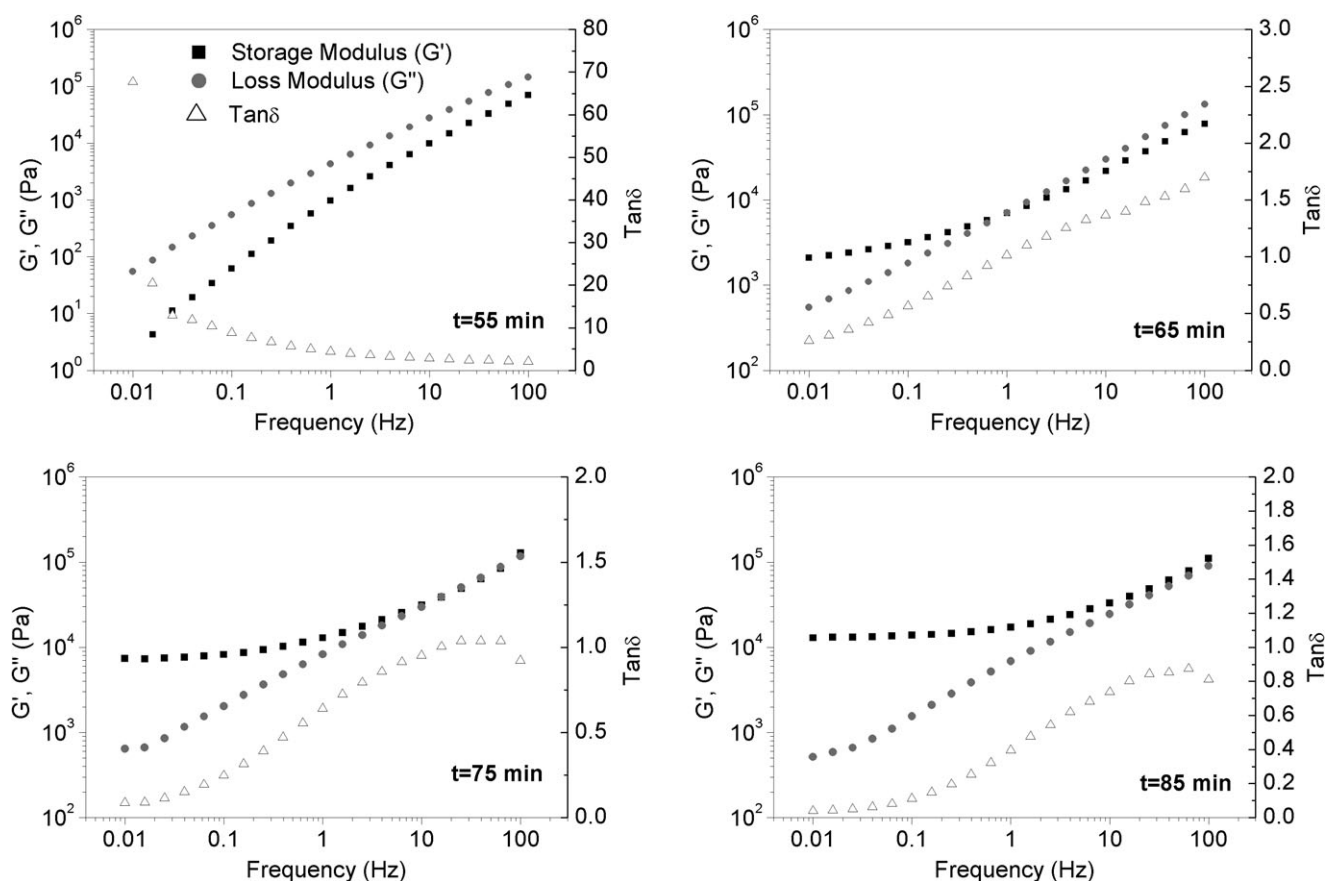


**Fig. 4** Rheological profile of ESO-SA samples cured at different times ( $R = 1$ ):  $G'$ ,  $G''$ , and  $\tan \delta$  vs. frequency

frequencies ( $G'' > G'$ ). Since the bonding frequency of the tack tests is in the vicinity of  $1\text{--}10^{-1} \text{ s}^{-1}$  frequency (Chang, 1991), the relatively high viscous component at 1 Hz ( $G' = G''$  at approximately 1 Hz) suggests that the PSA will dissipate high energy through deformation, suggesting a good performance as permanent PSA (Creton, 2003). This result is in agreement with the higher cross-linking degree of this sample (gel content =  $63.3 \pm 3.0\%$ ).

Still increasing curing time up to 75 min resulted in gels with higher cohesion but less tackiness than those cured for 65 min. Again, the behavior was dependent on the frequency showing an elastic behavior ( $G' > G''$ ) at low frequencies and a viscous behavior at high frequencies, unless crossover took place at much higher frequency (approximately 10 Hz). Loss modulus at 1 Hz was approximately 25% of  $G'$ . This reduction in the value of  $G''$  relative to  $G'$  implies that crack propagation becomes less dissipative and fibrillation is minimized, suggesting good performance as removable PSA (Creton, 2003). Finally, samples cured longer times, ca. 85 min, were cohesive rubber-like gels with very little or no tack at touch. As shown in Fig. 4, these samples exhibited an elastic behavior ( $G' > G''$ ) in the studied frequency range, being the curve of Cole-Cole plot located on the right side

of the equimoduli limit (Fig. 5b). Higher cross-linking led to samples with no crack blunting, that probably lack the viscous behavior needed for PSA applications.

## Conclusions

Completely bio-based PSA formulations with tailored viscoelastic properties were obtained from ESO and SA, both derived from plant oils. Synthesis was performed by a sustainable and environmentally sound one-pot procedure by reacting ESO and SA in the absence of any additional chemicals such as volatile solvents and catalysts. Curing conditions, pot-life, and gel content were determined. The rheological profile and gel content of the obtained PSA were greatly dependent on the curing conditions (temperature and time). ESO-SA stoichiometric mixtures cured at  $170^\circ\text{C}$  between 65 and 75 min showed the best balance between tack and cohesion. Based on these results, it can be concluded that the viscoelastic profile, cohesion, and adhesive properties of ESO-SA-based PSA can be tailored by controlling the curing parameters according to the desired application (i.e., permanent or removable PSA).

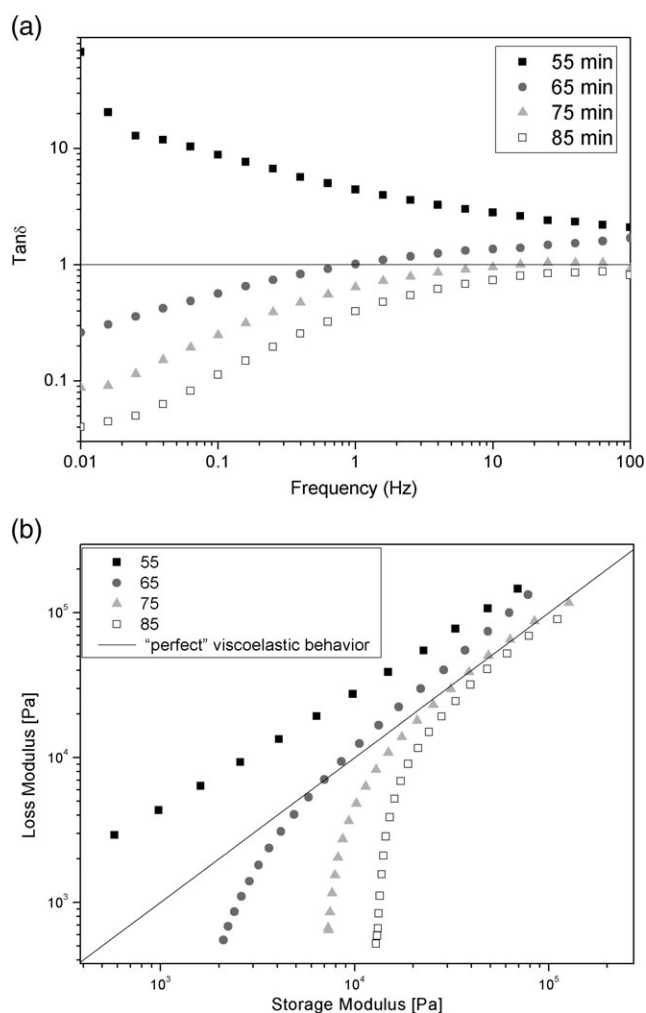


**Fig. 5** Comparison of rheology results of ESO-SA samples cured at different times ( $R = 1$ ): (a)  $\tan \delta$  vs. frequency and (b) Cole-Cole plots of all samples ( $G''$  vs.  $G'$ ). The line indicates the “perfect” viscoelastic behavior ( $G' = G''$ )

**Acknowledgments** The authors want to express their gratitude to Consejo Nacional de Investigaciones Científicas y Técnicas (CONICET) and Agencia Nacional de Promoción Científica y Tecnológica (ANPCyT, grant numbers PICT2015-1024 and PICT2013-0420) of Argentina for their financial support. Special thanks to Eng. Ulises Casado for his help in the rheological measurements.

**Conflict of Interest** The authors declare that they have no conflicts of interest.

## References

- Ahn, B. K., Kraft, S., Wang, D., & Sun, X. S. (2011) Thermally stable, transparent, pressure-sensitive adhesives from epoxidized and dihydroxyl soybean oil. *Biomacromolecules*, **12**:1839–1843.
- Ahn, B. K., Sung, J., Kim, N., Kraft, S., & Sun, X. S. (2013) UV-curable pressure-sensitive adhesives derived from functionalized soybean oils and rosin ester. *Polymer International*, **62**:1293–1301.
- Altuna, F., Espósito, L., Ruseckaite, R., & Stefani, P. (2011) Thermal and mechanical properties of anhydride-cured epoxy resins with different contents of biobased epoxidized soybean oil. *Journal of Applied Polymer Science*, **120**:789–798.
- Auvergne, R., Caillol, S., David, G., Boutevin, B., & Pascault, J.-P. (2013) Biobased thermosetting epoxy: Present and future. *Chemical Reviews*, **114**:1082–1115.
- Chang, E. (1991) Viscoelastic windows of pressure-sensitive adhesives. *The Journal of Adhesion*, **34**:189–200.
- Cohen, E., Binshtok, O., Dotan, A., & Dodiuk, H. (2013) Prospective materials for biodegradable and/or biobased pressure-sensitive adhesives: A review. *Journal of Adhesion Science and Technology*, **27**:1998–2013.
- Creton, C. (2003) Pressure-sensitive adhesives: An introductory course. *MRS Bulletin*, **28**:434–439.
- de Espinosa, L. M., & Meier, M. A. (2011) Plant oils: The perfect renewable resource for polymer science?! *European Polymer Journal*, **47**:837–852.
- Ding, C., & Matharu, A. S. (2014) Recent developments on biobased curing agents: A review of their preparation and use. *ACS Sustainable Chemistry & Engineering*, **2**:2217–2236.
- Ding, C., Shuttleworth, P. S., Makin, S., Clark, J. H., & Matharu, A. S. (2015) New insights into the curing of epoxidized linseed oil with dicarboxylic acids. *Green Chemistry*, **17**:4000–4008.
- Gay, C., & Leibler, L. (1999) On stickiness. *Physics Today*, **52**:48–52.
- Li, A., & Li, K. (2014a) Pressure-sensitive adhesives based on soybean fatty acids. *RSC Advances*, **4**:21521–21530.
- Li, A., & Li, K. (2014b) Pressure-sensitive adhesives based on epoxidized soybean oil and dicarboxylic acids. *ACS Sustainable Chemistry & Engineering*, **2**:2090–2096.
- Li, A., & Li, K. (2015) Pressure-sensitive adhesives based on tung oil. *RSC Advances*, **5**:85264–85271.
- Li, Y., Chou, S.-H., Qian, W., Sung, J., Chang, S. I., & Sun, X. S. (2017) Optimization of soybean oil based pressure-sensitive adhesives using a full factorial design. *Journal of the American Oil Chemists' Society*, **94**:713–721.
- Li, Y., & Sun, X. S. (2014) Di-hydroxylated soybean oil polyols with varied hydroxyl values and their influence on UV-curable pressure-sensitive adhesives. *Journal of the American Oil Chemists' Society*, **91**:1425–1432.
- Li, Y., & Sun, X. S. (2015) Synthesis and characterization of acrylic polyols and polymers from soybean oils for pressure-sensitive adhesives. *RSC Advances*, **5**:44009–44017.
- Li, Y., Wang, D., & Sun, X. S. (2015) Copolymers from epoxidized soybean oil and lactic acid oligomers for pressure-sensitive adhesives. *RSC Advances*, **5**:27256–27265.
- Maaßen, W., Oelmann, S., Peter, D., Oswald, W., Willenbacher, N., & Meier, M. A. (2015) Novel insights into pressure-sensitive adhesives based on plant oils. *Macromolecular Chemistry and Physics*, **216**:1609–1618.
- Maassen, W., Meier, M. A., & Willenbacher, N. (2016) Unique adhesive properties of pressure sensitive adhesives from plant oils. *International Journal of Adhesion and Adhesives*, **64**:65–71.
- Mashouf Roudsari, G., Mohanty, A. K., & Misra, M. (2014) Study of the curing kinetics of epoxy resins with biobased hardener and epoxidized soybean oil. *ACS Sustainable Chemistry & Engineering*, **2**:2111–2116.
- Torron, S., Hult, D., Pettersson, T., & Johansson, M. (2017) Tailoring soft polymer networks based on sugars and fatty acids toward pressure sensitive adhesive applications. *ACS Sustainable Chemistry & Engineering*, **5**:2632–2638.

- Vendamme, R., & Eevers, W. (2013) Sweet solution for sticky problems: Chemoreological design of self-adhesive gel materials derived from lipid biofeedstocks and adhesion tailoring via incorporation of isosorbide. *Macromolecules*, **46**:3395–3405.
- Vendamme, R., Olaerts, K., Gomes, M., Degens, M., Shigematsu, T., & Eevers, W. (2012) Interplay between viscoelastic and chemical tunings in fatty-acid-based polyester adhesives: Engineering biomass toward functionalized step-growth polymers and soft networks. *Biomacromolecules*, **13**:1933–1944.
- Wang, X.-L., Chen, L., Wu, J.-N., Fu, T., & Wang, Y.-Z. (2017) Flame-retardant pressure-sensitive adhesives derived from epoxidized soybean oil and phosphorus-containing dicarboxylic acids. *ACS Sustainable Chemistry & Engineering*, **5**:3353–3361.
- Wool, R. P. (2013) 12 - Pressure-sensitive adhesives, elastomers, and coatings from plant oil A2. In S. Ebnesajjad (Ed.), *Handbook of biopolymers and biodegradable plastics* (pp. 265–294). Boston: William Andrew Publishing. <https://doi.org/10.1016/B978-1-4557-2834-3.00012-4>
- Wu, Y., Li, A., & Li, K. (2014) Development and evaluation of pressure sensitive adhesives from a fatty ester. *Journal of Applied Polymer Science*, **131**:41143. <https://doi.org/10.1002/app.41143>
- Wu, Y., Li, A., & Li, K. (2015) Pressure sensitive adhesives based on oleic acid. *Journal of the American Oil Chemists' Society*, **92**: 111–120.
- Wu, Y., & Li, K. (2016) Replacement of styrene with acrylated epoxidized soybean oil in an unsaturated polyester resin from propylene glycol, isophthalic acid, and maleic anhydride. *Journal of Applied Polymer Science*, **133**:43052. <https://doi.org/10.1002/app.43052>
- Wu, Y., & Li, K. (2017) Replacement of styrene with acrylated epoxidized soybean oil in an unsaturated polyester resin from propylene glycol and maleic anhydride. *Journal of Applied Polymer Science*, **134**:45056. <https://doi.org/10.1002/app.45056>
- Zeng, R.-T., Wu, Y., Li, Y.-D., Wang, M., & Zeng, J.-B. (2017) Curing behavior of epoxidized soybean oil with biobased dicarboxylic acids. *Polymer Testing*, **57**:281–287.